Tetrahedron **1996**, *52*, 5065 – 5075; c) F. Djojo, E. Ravanelli, O. Vostrowsky, A. Hirsch, *Eur. J. Org. Chem.* **2000**, 1051 – 1059.
[12] a) L. Isaacs, P. Seiler, F. Diederich, *Angew. Chem.* **1994**, *106*, 2434 – 2437; *Angew. Chem. Int. Ed. Engl.* **1994**, *33*, 2339 – 2342; b) L. Isaacs, F. Diederich, R. F. Haldimann, *Helv. Chim. Acta* **1997**, *80*, 317 – 342; c) J. F. Nierengarten, T. Habicher, R. Kessinger, F. Cardullo, F. Diederich, V. Gramlich, J. P. Gisselbrecht, C. Boudon, M. Gross, *Helv. Chim. Acta* **1997**, *80*, 2238 – 2276; d) F. Cardullo, P. Seiler, L. Isaacs, J. F. Nierengarten, R. F. Haldimann, F. Diederich, T. Mordasini-Denti, W. Thiel, C. Boudon, J. P. Gisselbrecht, M. Gross, *Helv. Chim. Acta* **1997**, *80*, 343 – 371; e) F. Diederich, R. Kessinger, *Acc. Chem. Res.* **1999**, *32*, 537 – 545, and references therein.
[13] W. Qian, Y. Rubin, *Angew. Chem.* **1999**, *111*, 2504 – 2508; *Angew. Chem. Int. Ed.* **1999**, *38*, 2356 – 2360.
[14] The term "regioisomer" for fullerene adducts is somewhat vague because it can refer to both positional isomers (e.g., *cis*-1, *cis*-2, *cis*-3, *e*′, *e*″, *trans*-1, *trans*-2, *trans*-3, *trans*-4 bisadducts) and "permutational" isomers as is the case here. We are tentatively using the latter term to refer to the permutations that are need to "exchange" addends between the different regioisomers within the T_h framework.
[15] The term *mer* is used in analogy to the corresponding topology in octahedral transition metal complexes.
[16] a) S. Y. Ko, A. W. M. Lee, S. Masamune, L. A. Reed III, K. B. Sharpless, F. J. Walker, *Science* **1983**, *220*, 949 – 951; b) S. Y. Ko, A. W. M. Lee, S, Masamune, L. A. Reed III, K. B. Sharpless, F. J. Walker, *Tetrahedron* **1990**, *46*, 245 – 264.
[17] For experimental data, see the Supporting Information.
[18] Y.-Z. An, G. A. Ellis, A. L. Viado, Y. Rubin, *J. Org. Chem.* **1995**, *60*, 6353 – 6361.
[19] X. Camps, A. Hirsch, *J. Chem. Soc. Perkin Trans. 1* **1997**, 1595 – 1596.
[20] J.-M. Lehn, *Supramolecular Chemistry*, VCH, Weinheim, **1995**.
[21] T. DaRos, M. Prato, *Chem. Commun.* **1999**, 663 – 669.

A Chip-Based Biosensor for the Functional Analysis of Single Ion Channels**

Christian Schmidt,* Michael Mayer, and Horst Vogel*

The functional analysis of single ion channel proteins presents a serious bottleneck in the process of finding new pharmacologically active compounds. Single channel recording methods currently available (patch clamp,[1] black lipid membrane (BLM)[2]) are not suited for automation and miniaturization. However, new techniques such as combinatorial chemistry[3] and combinatorial genetics,[4] which produce large numbers of potential drugs and mutant proteins, respectively, demand efficient and reliable high-throughput screening (HTS) as well as low sample consumption.[5] In this context, monitoring the current of single ionotropic receptors with automated biosensor devices may result in new classes of highly sensitive screening tools.

Functional studies of single ion channel proteins require the reduction of electrical background noise to 10^{-13} – 10^{-12} A and consequently a high electrical insulation of the surrounding membrane patch ($R > 10^9\ \Omega$, "giga-seal") under conditions of low dielectric loss and low electrical capacitance.[1] Classically, tight seals are obtained manually by suction of small membrane patches (from cells or proteoliposomes) into glass micropipettes[6] or by "painting" of lipid bilayers across holes in teflon septa.[2, 7]

Single-channel recording systems suited for biosensor and HTS applications require a new approach. The self-positioning of unilamellar lipid vesicles on planar insulating diaphragms presents one solution. Since the surface of most native membrane vesicles and cells bears electrical charges,[8] properly directed electrical fields can provide precise electrophoretic positioning. However, efficient electrophoretic attraction of vesicles can only be realized for electrokinetic velocities v_{ek} (vesicle) $\gg 1\ \mu m\,s^{-1}$, which requires electric fields of several hundred volts per meter.[9] In a homogeneous field, such field strengths are only obtained under unfavorable conditions such as high voltages or very short electrode distances. Consequently, strongly inhomogeneous fields were used for positioning, which resulted in a focused movement of vesicles towards the point with the highest voltage gradient.

An inhomogeneous electrical field (Figure 1a) was created around a small aperture located in a thin insulating diaphragm (Figure 1b) separating two fluid compartments. By accessing both compartments with low impedance redox electrodes (Figure 1c) the main voltage drop after application of a potential V_C occurred within and near the aperture (Figure 1a). The resulting radially symmetrical field E directed the electrophoretic movement of charged objects to the spatially fixed aperture. The geometry of the aperture and the limitation of the applied voltage V_C to physiological potentials (< 200 mV, to avoid artifacts such as electroporation after seal formation) define the strength of the electric field. Optimal conditions for positioning were obtained by reducing the diaphragm thickness h to the minimum size that would provide sufficient stability and insulation ($h \approx 100$ nm) and by adaptation of the aperture diameter to the vesicle size ($d_A = 0.6 – 7\ \mu m$). Figure 1a illustrates that under optimal conditions the "electrophoretic trap" extends less than 20 μm into the buffer volume. Despite this short attractive range vesicles frequently enter the electrophoretic trap by convection during vesicle addition or by sedimentation within the small volume of the compartment (1 – 10 μL, Figure 2a).

The feasibility of electrophoretic focusing was demonstrated using negatively charged giant unilamellar vesicles (Figure 2b) and bare silicon nitride diaphragms. Within 1 – 10 s after the addition to the *cis* compartment (Figure 1c, upper side), vesicles were trapped and moved through the aperture. The resulting current modulations (Figure 2a) resembled Coulter-counter events ($V_c = 80$ mV).[10] Even vesicles larger

[*] Dr. C. Schmidt,[+] Prof. Dr. H. Vogel, M. Mayer
Institute of Physical Chemistry
Swiss Federal Institute of Technology
1015 Lausanne (Switzerland)
Fax: (+41) 21-693-6190
E-mail: horst.vogel@epfl.ch

[+] Present address
CYTION SA, Biopole
Chemin des Croisettes 22
1066 Epalinges (Switzerland)
Fax: (+41) 21-693-8426
E-mail: christian.schmidt@cytion.com

[**] We thank E. Ermanntraut, L. Giovangrandi, T. Wohland, A. Brecht, M. Köhler, C. Bieri, D. Stamou, and R. Hovius for advice. This work was supported by the Swiss National Science Foundation (Priority Program for Biotechnology) and by an interdepartmental grant of the Swiss Federal Institute of Technology Lausanne (EPFL, Project Microtechnique 96).

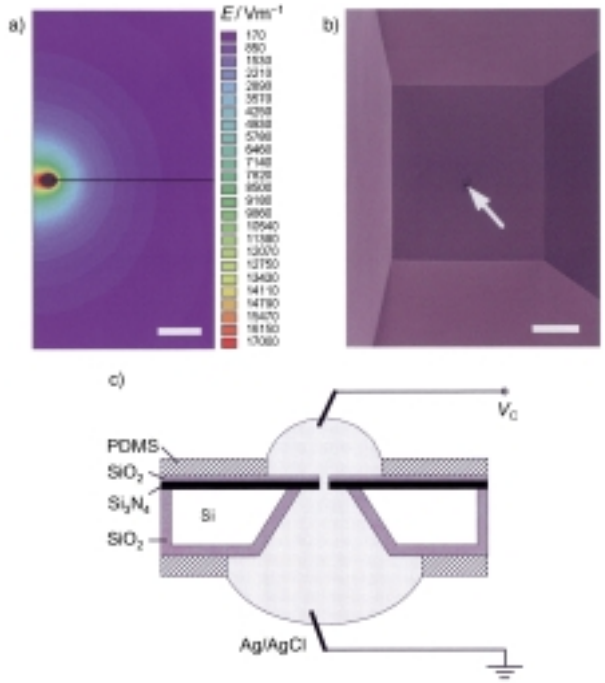

Figure 1. Characteristics of the planar recording setup. a) The electric field E near the aperture of the diaphragm mediates the electrophoretic movement of charged objects within a distance of several micrometers. The field outside the aperture along its center axis was approximated by:

$$E(L,d_A,h) = \frac{V_C \cdot d_A^3}{(h+d_A)\,(d_A^2+4L^2)^{3/2}},$$

assuming E is constant inside the aperture and $L \to \infty$ for the position of the electrodes (L = distance from the center of the aperture surface).[24] A finite element simulation of the spatial-field distribution around a 4-μm aperture (axis of rotation to the left) for plane-parallel electrodes located 1 mm opposite the diaphragm is shown ($V_C = -100$ mV, diaphragm thickness $h = 100$ nm, scale bar: 4 μm). Near the rim E exceeds 17000 V m^{-1} and is shown in gray. b) Scanning electron micrograph showing the Si_3N_4 diaphragm and the aperture (see arrow) at the bottom of a pyramidal well. The low dielectric loss factor of $D \le 10^{-4}$ and the high electric resistivity of $\rho > 10^{12}$ Ωm for Si_3N_4 allowed the diaphragm thickness to be reduced to $h = 100-150$ nm (scale bar: 25 μm, tilt = 30°). c) Schematic diagram of the recording setup. A fluid compartment was etched into a 400-μm thick silicon chip. The Si_3N_4 diaphragm contained an aperture with a diameter between 0.6 and 7 μm. The chip (cross section) was sandwiched between two polydimethylsiloxane (PDMS) elastomer pads, which provided access to the diaphragm and confined the free-standing recording compartments. The compartment volume was usually about 10 μL but can be reduced to 1 μL. Ag/AgCl redox electrodes were used for voltage application during electrophoretic positioning and for subsequent voltage clamp recordings. The distance and placement of the electrodes was not important, since the main voltage drop occurred across the aperture. An additional SiO_2 layer (thickness ca. 1 μm) was grown on the silicon bulk to reduce the capacitance ($C < 35$ pF) and consequently the capacitive noise to $\sigma < 200$ fA rms. The series resistance was between 80 to 280 kΩ in 85 mM KCl.

than the aperture passed through the unmodified Si_3N_4 diaphragm as indicated by the dwell-time distribution.

Tight and permanent binding of vesicles to the diaphragm is required for the measurement of single ion channel currents. A sufficiently close contact between the diaphragm surface and lipid membrane can be mediated by electrostatic forces.[11] In order to exploit electrostatic attraction 20 nm of SiO_2 was deposited on the Si_3N_4 diaphragm, which was either chemically modified with 4-aminobutyldimethylmethoxysilane or covered by physisorbed poly-L-lysine.[12] The resulting positive charges on the surface within the aqueous recording environment caused a spontaneous and stable reduction in the current after the positioning of a negatively charged giant vesicle. This indicates vesicle fusion to the highly attractive diaphragm surface (Figures 2c and d). After formation of the

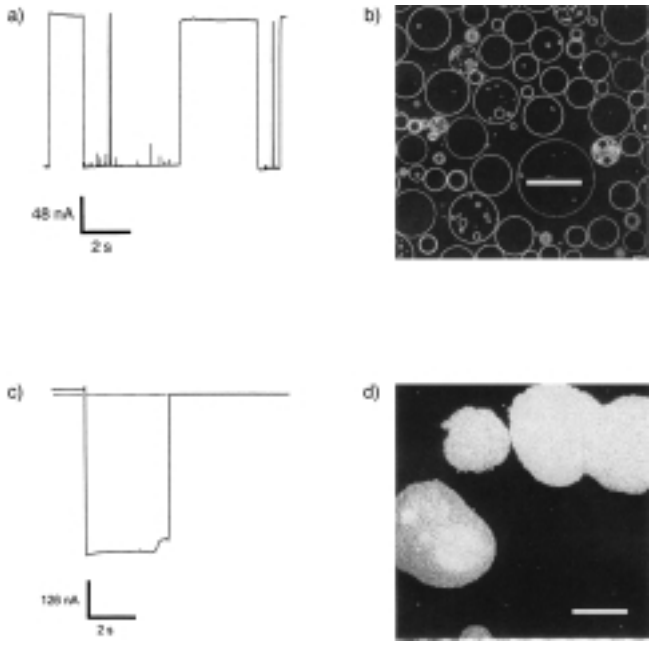

Figure 2. Voltages of $V_C < |150$ mV$|$ were sufficient to trap giant unilamellar vesicles. a) At negative potentials, vesicles added to the *cis* side of a bare Si_3N_4 diaphragm were electrophoretically trapped and moved to the opposite compartment ($h = 100-150$ nm, $d_A = 7$ μm). The current modulations $I(t) = V_C R(t)^{-1}$ are shown, which were caused by vesicles moving through the aperture and which depended on the vesicle size and concentration. Reversing the field orientation retracted previously passed vesicles into the *cis* compartment. b) The laser scanning microscopic (LSM) image of fluorescently labeled vesicles after size purification using a nylon net with a mesh size of 20 μm (scale bar: 50 μm). c) As in (a) but with a positively charged Si_3N_4/SiO_2 diaphragm (4-aminobutyldimethylmethoxysilane). Vesicles spread instantaneously on the highly attractive diaphragm surface forming GΩ seals without the need for manual control ($R = 83$ GΩ, dashed line: $I(t) = 0$ pA). In contrast to traditional BLM experiments,[2] vesicle-derived planar bilayers are solvent-free. d) The LSM image of giant vesicles fused to the SiO_2 surface (scale bar: 50 μm). The formation of single-layered membranes was promoted by the strong electrostatic interaction between vesicles and diaphragm and by osmotic stress of the vesicles (vesicles filled with 200 mM sorbitol added to the *cis* compartment containing 85 mM KCl).

seal, the major voltage drop occurred across the newly built membrane patch. The corresponding field reduction outside the membrane patch automatically stopped the electrophoretic movement of additional vesicles. Seal resistances varied from $R = 1.4$ to 74 GΩ (poly-L-lysine) and $R = 9$ to > 200 GΩ (4-aminobutyldimethylmethoxysilane). In contrast to patch clamp techniques, calcium ions were not required in the buffer for formation of the seal. This result opens up the possibility of varying the concentration of Ca^{2+} ions and therefore performing detailed studies on calcium-dependent membrane processes.[13]

The efficient formation of seal resistances of $R > 10^9$ Ω required vesicles with diameters at least three times greater

  0044-8249/00/11217-3268 $ 17.50+.50/0

than the aperture size. The presence of significantly smaller vesicles presumably resulted in small negatively charged surface zones, which impaired the tight adhesion of hole-spanning giant vesicles. Stable membranes on the chip with seal resistances of $R > 10^9\ \Omega$ were obtained in 99 out of 134 experiments after removal of small vesicles by dialysis (20 μm mesh size). The membranes were usually stable for more than 60 min in 10 – 500 mM KCl and 0 – 4 mM $CaCl_2$.

Information about the structure of negatively charged vesicle membranes after adhesion to positively charged surfaces was obtained by scanning confocal fluorescence microscopy using fluorescently labeled vesicles. Complete binding of vesicles occurred instantaneously after sedimentation of the vesicles to the surface. The resulting membrane patches were extremely flat (thickness < 0.8 μm, below the z-resolution of the microscope) and correlated in size to the surface area of vesicles in solution ($3293 \pm 692 : 3300 \pm 165\ \mu m^2$, $n = 34$), which suggests the formation of planar unilamellar bilayers (in contrast to an expected ratio of 1:2 for two adjacently layered membranes of intact but flattened vesicles). The observed formation of single bilayers upon spreading giant, osmotically stressed vesicles on highly attractive surfaces is in agreement with previously described work.[11]

Planar unilamellar membranes on low capacitance silicon chips ($C < 35$ pF) are ideally suited for low noise electrical recording of transmembrane ion currents. The general functionality of this new concept was demonstrated with alamethicin, a peptide known to self-integrate into bilayers and to form voltage-gated ion channels of defined conductance by oligomerization.[2, 14] The voltage-dependent activation of single alamethicin channels with up to seven conductance states was observed (Figures 3a and b) 10 – 150 s after adding the peptide (final concentration, 2.5 ng mL^{-1}) to the *cis* side of a vesicle-derived planar bilayer.[15] The dwell-time distribution and the nearly symmetrical current – voltage relationship derived from these events are typical for the activation of alamethicin in asolectin membranes.[2, 16] Changing the lipid composition to include 45% 1-palmitoyl-2-oleoyl-*sn*-glycero-3-phosphoethanolamine (POPE) and 25% cholesterol restricted the channel activation to positive potentials, as previously reported.[16]

In this work we have shown that stable gigaohm seals over micrometer-sized holes can be obtained in a time-frame of seconds by the electrophoretic self-positioning of charged lipid membranes. For the first time, single-channel events were recorded on silicon microstructures. Self-integrating channel-forming peptides, such as alamethicin and gramicidin,[17] or pore-forming proteins, such as α-haemolysin[18] and OmpF,[19] are expected to have applications in screening assays based on single-channel recordings, including high-speed DNA sequencing[20] and metabolite detection. In the future, this method could be extended by either functional reconstitution of ion channels into giant vesicles[21] or their fusion (small proteoliposomes) into preformed bilayers.[7, 22] The possibility of combining this type of planar set-up with high numerical optics may also enable the simultaneous observation of electrical and optical signals, which would help to elucidate the coupling between ligand-binding and channel events of ionotropic receptors.[23]

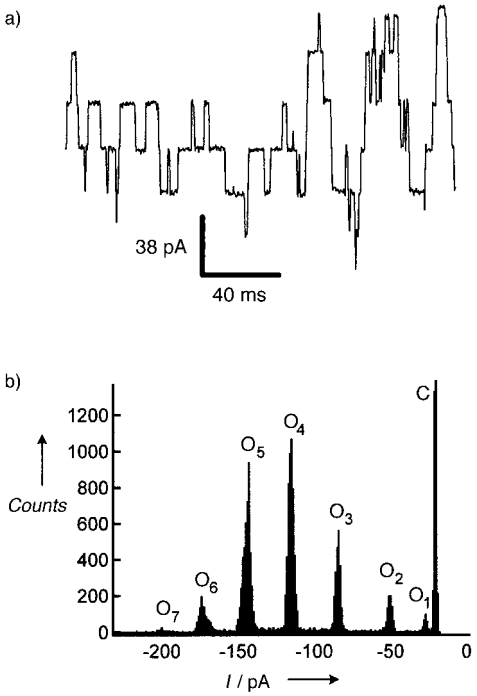

Figure 3. Voltage-dependent activation of single alamethicin channels. a) The I versus t diagram recorded at $V_C = -130$ mV in 0.2 M KCl and 8 mM HEPES, at pH 7.4 shows the typical activation pattern comprising up to seven conductance states. b) Current histogram derived from alamethicin traces recorded under conditions given in (a). The conductance states O_1 to O_7 are shown. C reflects the current baseline with the channel closed.

Recording chips can be produced in large numbers with defined geometry and material properties by standard silicon technology. Multiple recording sites can be integrated on one single chip because of the small lateral size of the diaphragm (less than 0.1 mm^2). The combination of silicon technology with the demonstrated principles of fast and reliable self-formation of low noise recording membranes in small sample volumes of 1 – 10 μL offers a unique approach for the realization of multiarray biosensors based on natural or designed[18] channel-forming peptides or ion channel proteins, as well as for large-scale functional screening in fundamental research and drug discovery.

Experimental Section

Chips ($3 \times 3 \times 0.5$ mm^3, Si wafer, (100) orientation, covered by a 0.1 – 1-μm thick plasma enhanced chemical vapor deposition (PECVD) Si_3N_4 layer) were structured by a combination of anisotropic KOH silicon etching and reactive-ion etching of the aperture. The anisotropic etching process was stopped at the Si_3N_4 layer, and resulted in a free-standing Si_3N_4 diaphragm of $10^{-9} - 10^{-8}$ m^2, into which the hole was etched. For chemical and physical modifications of the diaphragm, a 20-nm SiO_2 PECVD layer was deposited onto the Si_3N_4 surface. To reduce the capacitance an additional insulating SiO_2 layer (thickness ≥ 1 μm) was grown by thermal oxidation onto the silicon.

Positively charged diaphragm surfaces were prepared by incubating the chips either for ≥ 5 min in 0.1% poly-L-lysine (relative molecular mass $M_r = 70 - 150$ K) solution or overnight in dry toluene containing 1% of 4-aminobutyldimethylmethoxysilane.

Giant unilamellar vesicles were prepared by overnight swelling of vacuum-dried lipid films (1.25 mg total lipid) of either 70% asolectin, 25% 1-palmitoyl-2-oleoyl-*sn*-glycero-3-[phospho-*rac*-(1-glycerol)] (POPG), 5% cholesterol or 45% POPE, 25% cholesterol, 22.5% 1-palmitoyl-2-oleoyl-*sn*-glycero-3-phosphocholine (POPC), 7.5% POPG in deionized water

(10 mL) containing sorbitol (200 – 1000 mM). Lipid bilayers were labeled with *N*-(6-tetramethylrhodaminethiocarbamoyl)-1,2-dihexadecanoyl-*sn*-glycero-3-phosphoethanolamine (TRITC-DHPE, 0.07 %). The vesicles in solution and fused to surfaces were observed with a laser scanning microscope (Zeiss, LSM 510, Zeiss 60x/1.25 apochromat water immersion objective, pinhole size 100 μm) on either poly-L-lysine or 4-aminobutyldimethylmethoxysilane-modified glass coverslips coated with a 50 nm PECVD-SiO_2 layer.

Standard experiments were performed in 85 mM KCl, 2 mM *N*-(2-hydroxyethyl)piperazine-*N*′-(2-ethanesulfonic acid) (HEPES), at pH 7.4 using vesicles filled with 200 mM of sorbitol.

Received: April 27, 2000 [Z 15051]

[1] O. P. Hamill, A. Marty, E. Neher, B. Sakmann, F. J. Sigworth, *Pflügers Arch.* **1981**, *391*, 85.

[2] W. R. Schlue, W. Hanke, *Planar Lipid Bilayers*, Academic Press, London, **1993**.

[3] a) G. Jung, *Combinatorial Chemistry. Synthesis*, *Analysis*, *Screening*, Wiley-VCH, Weinheim, **1999**; b) J. Rademann, G. Jung, *Science* **2000**, *287*, 1947.

[4] a) M. Eigen, R. Rigler, *Proc. Natl. Acad. Sci. USA* **1994**, *91*, 5740; b) J. Hanes, L. Jermutus, S. Weber-Bornhauser, H. R. Bosshard, A. Plückthun, *Proc. Natl. Acad. Sci. USA* **1998**, *95*, 14130.

[5] J. Denyer, J. Worley, B. Cox, G. Allenby, M. Banks, *Drug Discovery Today* **1998**, *3*, 323.

[6] B. Sackmann, E. Neher, *Single-Channel Recording*, Plenum, New York, **1983**.

[7] H. Schindler, *Methods Enzymol.* **1989**, *171*, 225.

[8] R. B. Gennis, *Biomembranes*, Springer, New York, **1989**.

[9] A. Balasubramanian, S. McLaughlin, *Biochim. Biophys. Acta* **1982**, *685*, 1.

[10] P. Mueller, T. F. Chien, B. Rudy, *Biophys. J.* **1983**, *44*, 375.

[11] E. Sackmann, *Science* **1996**, *271*, 43.

[12] B. S. Jacobson, D. Branton, *Science* **1977**, *195*, 302.

[13] B. Hille, *Ionic Channels of Excitable Membranes 2nd ed.*, Sinauer, Sunderland, **1992**.

[14] G. Boheim, W. Hanke, G. Jung, *Biophys. Struct. Mech.* **1983**, *9*, 181.

[15] W. Hanke, G. Boheim, *Biochim. Biophys. Acta* **1980**, *596*, 456.

[16] I. Vodyanoy, J. E. Hall, T. M. Balasubramanian, *Biophys. J.* **1983**, *42*, 71.

[17] a) B. A. Cornell, V. L. Braach-Maksvytis, L. G. King, P. D. Osman, B. Raguse, L. Wieczorek, R. J. Pace, *Nature* **1997**, *387*, 580; b) P. Fromherz, V. Kiessling, K. Kottig, G. Zeck, *Appl. Phys. A* **1999**, *69*, 571; c) S. M. Bezrukov, I. Vodyanoy, V. A. Parsegian, *Nature* **1994**, *370*, 279.

[18] a) L. Q. Gu, O. Braha, S. Conlan, S. Cheley, H. Bayley, *Nature* **1999**, *398*, 686; b) M. Pawlak, U. Meseth, B. Dhanapal, M. Mutter, H. Vogel, *Protein Sci.* **1994**, *3*, 1788.

[19] T. Stora, J. H. Lakey, H. Vogel, *Angew. Chem.* **1999**, *111*, 402; *Angew. Chem. Int. Ed.* **1999**, *38*, 389.

[20] a) D. W. Deamer, M. Akeson, *Trends Biotechnol.* **2000**, *18*, 147; b) A. Meller, L. Nivon, E. Brandin, J. Golovchenko, D. Branton, *Proc. Natl. Acad. Sci. USA* **2000**, *97*, 1079; c) J. J. Kasianowicz, E. Brandin, D. Branton, D. W. Deamer, *Proc. Natl. Acad. Sci. USA* **1996**, *93*, 13770; d) D. Branton, J. Golovchenko, *Nature* **1999**, *398*, 660.

[21] a) B. U. Keller, R. Hedrich, W. L. Vaz, M. Criado, *Pfluegers Arch.* **1988**, *411*, 94; b) A. Moscho, O. Orwar, D. T. Chiu, B. P. Modi, R. N. Zare, *Proc. Natl. Acad. Sci. USA* **1996**, *93*, 11443; c) G. Riquelme, E. Lopez, L. M. Garcia-Segura, J. A. Ferragut, J. M. Gonzalez-Ros, *Biochemistry* **1990**, *29*, 11215; d) M. Criado, B. U. Keller, *FEBS Lett.* **1987**, *224*, 172; e) H. Kawai, L. Cao, S. M. Dunn, W. F. Dryden, M. A. Raftery, *Biochemistry* **2000**, *39*, 3867.

[22] a) G. Boheim, W. Hanke, F. J. Barrantes, H. Eibl, B. Sakmann, G. Fels, A. Maelicke, *Proc. Natl. Acad. Sci. USA* **1981**, *78*, 3586; b) C. Miller, *Physiol. Rev.* **1983**, *63*, 1209.

[23] a) S. J. Edelstein, O. Schaad, J. P. Changeux, *Biochemistry* **1997**, *36*, 13755; b) S. Weiss, *Science* **1999**, *283*, 1676; c) A. Cha, G. E. Snyder, P. R. Selvin, F. Bezanilla, *Nature* **1999**, *402*, 809; d) L. M. Mannuzzu, M. M. Moronne, E. Y. Isacoff, *Science* **1996**, *271*, 213.

[24] J. D. Jackson, *Klassische Elektrodynamik*, 2nd ed., de Gruyter, Berlin, **1982**.

A Room-Temperature Discotic Nematic Liquid Crystal**

Sandeep Kumar* and Sanjay Kumar Varshney

Liquid crystal displays (LCDs) have played a vital role in information technology. The twisted nematic and supertwisted nematic display devices have dominated commercial displays since their invention. The liquid crystal layer in these devices is made up exclusively of calamitic liquid crystals (composed of rod-shaped molecules). A number of calamitic nematic liquid crystals having room-temperature mesophases—such as, cyanobiphenyls, phenylpyrimidines, phenylcyclohexanes, and Schiff bases—have been synthesized and used in practical displays.[1, 2]

The major disadvantage with these types of devices is the narrow and nonuniform viewing cone, which is considered to be an unacceptable aspect of their performance. Several methods have been put forward to improve the viewing angle characteristics, for example the multidomain technique,[3] the introduction of an optical compensator to reduce the amount of light leakage in the dark state,[4] the application of an electric field parallel to the plane of the substrates,[5] and the "amorphous" twisted nematic liquid crystal displays (TNLCD).[6] We recently disclosed a novel approach to overcome this problem by utilizing discotic nematic liquid crystals instead of calamitic nematic liquid crystals.[7] Compared to the large number of calamitic molecules showing a nematic phase, there are only few disk-shaped molecules showing a discotic nematic phase N_D. Several derivatives of triphenylene,[8, 9] truxene,[10] thiotruxene,[11] and naphthalene[12] show stable discotic nematic phases, but these phases are high-temperature and narrow. For any application as a liquid crystal device, stability of the mesophase well below and above room temperature is one of the most important criteria.

Hitherto, no room-temperature discotic nematic liquid crystal was known. The common procedure for extending the mesophase range of calamitic liquid crystals is by mixing different components and preparing an eutectic mixture, but such a procedure has not been applied to discotic nematic till now. Therefore, it is of great practical interest to prepare room-temperature discotic nematic liquid crystals. Here we report on the synthesis of the first example of a room-temperature discotic nematic liquid crystal.

Hexa- and pentaalkynylbenzene derivatives having N_D phases have recently received a great deal of attention as their clearing temperatures are not very high and they show a chiral nematic-discotic phase on doping with suitable chiral molecules. Several hexa- and pentaalkynylbenzenes and their dimers were prepared and studied extensively.[9, 13]

When the peripheral alkyl chains are attached to the phenyl ring in the hexaalkynylbenzene derivatives through a hetero-

[*] Dr. S. Kumar, S. K. Varshney
Centre for Liquid Crystal Research
P.O. Box 1329, Jalahalli, Bangalore-560013 (India)
Fax: (+91) 80-838-2044
E-mail: uclcr@giasbg01.vsnl.net.in

[**] We are very grateful to Professor S. Chandrasekhar for helpful discussions.

  0044-8249/00/11217-3270 $ 17.50+.50/0